Organic Electronics

DOI: 10.1002/anie.200900472

Interactive Radical Dimers in Photoconductive Organic Thin Films**

Akito Iwasaki, Laigui Hu, Rie Suizu, Kenji Nomura, Hirofumi Yoshikawa, Kunio Awaga, Yukiko Noda, Kaname Kanai, Yukio Ouchi, Kazuhiko Seki, and Hiroshi Ito*

In recent years, organic semiconductors have received a new impetus in the field of organic electronics, which has been stimulated by the development of organic light-emitting diodes, field-effect transistors, and photovoltaic cells.[1] Work in this field, however, has focused almost entirely on closed-shell molecules, and scant attention has been paid to the use of molecules with unpaired electrons as building blocks for semiconducting thin films and associated devices. In contrast, many organic radicals have been extensively studied as crystalline conducting or magnetic materials, and it is now recognized that the unpaired electrons on these materials bring about unusual intermolecular interactions, intermolecular arrangements, and external magnetic field effects. Despite the presence of unpaired electrons as potential charge carriers, organic radicals always exhibit semiconductive behavior that arises from effects such as electron–electron correlations or electron–lattice interactions.[2–9] If such paramagnetic semiconductive materials are incorporated into organic electronic devices, it is expected that they will work under a very different operating principle.

In the solid state, organic radicals often exhibit a dimerized structure. When two π-radical molecules exhibit a face-to-face overlap, a bonding supramolecular orbital (BO) and an antibonding supramolecular orbital (ABO) are formed (Figure 1a). Note that the population of the BO is concentrated at the center of the dimer, while that of the ABO spreads outside along the R−R axis. If these radical dimers make stacking chains with π–π interactions, the ABOs are expected to make a wide band through a large interdimer overlap. We can therefore expect high photoconductivity by the electron migration in the wide ABO band (Figure 1b), in contrast to the insulating behavior in the ground state. In addition, the valence-bond picture suggests that the photoexcited state includes a charge-transfer character, namely $R{:}R \rightarrow R^{+}R^{-}$, which can be regarded as a precursor stage of charge separation. These "interactive radical dimers" are considered to be promising as they can exhibit photoactive behavior.

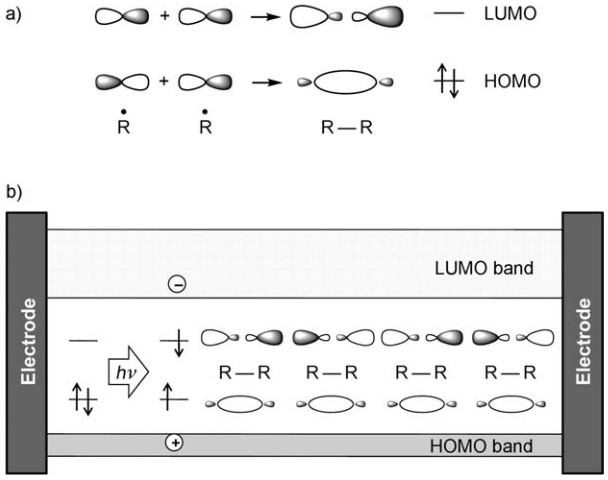

Figure 1. a) Bonding and antibonding supramolecular orbitals of the π-radical dimer. b) Result of photoexcitation of the HOMO and LUMO bands of interacting radical dimers.

A thiazyl diradical, 4,4′-bis(1,2,3,5-dithiadiazolyl)[10] (BDTDA, see the inset of Figure 2c) possesses ideal features to test the "interactive radical dimers" mechanism. The thiazyl radical family demonstrates chemical stability and strong intermolecular interactions, and has been shown to have various interesting properties.[11–16] Since BDTDA is a so-called disjoint diradical, the molecular orbitals for the two unpaired electrons are localized on separate five-membered rings and the exchange interactions between the two radical centers are very small.[10] The crystal structure of BDTDA in fact consists of a face-to-face BDTDA dimer, which reflects the fact that the intermolecular interaction is stronger than the intramolecular interaction. These dimers undergo π stacking along the monoclinic *a* axis, and the packing of dimeric stacks produces a herringbone-like motif with electrostatic $S^{\delta+}\cdots N^{\delta-}$ contacts, in which all the molecular planes of BDTDA are parallel to the *bc* plane (see the inset in Figure 2c; the highest occupied molecular orbital (HOMO) and lowest unoccupied molecular orbital (LUMO) of the BDTDA dimer, calculated from the crystal geometry are shown in Figure S1 in the Supporting Information).[10] Their features are quite similar to the schematic views shown in Figure 1a.

The out-of-plane XRD patterns of the BDTDA thin films deposited by vacuum vapor deposition on Si(100), indium tin

---

[*] A. Iwasaki, Dr. L. Hu, Dr. R. Suizu, K. Nomura, Dr. H. Yoshikawa, Prof. K. Awaga, Y. Noda, Dr. K. Kanai, Prof. Y. Ouchi, Prof. K. Seki
Research Center for Materials Science and
Department of Chemistry, Nagoya University
Furo-cho, Chikusa-ku, Nagoya 464-8602 (Japan)
Fax: (+81) 52-789-2487
E-mail: awaga@mbox.chem.nagoya-u.ac.jp
Homepage: http://www.chem.nagoya-u.ac.jp/awagak/index.html
Prof. H. Ito
Department of Applied Physics, Nagoya University
Furo-cho, Chikusa-ku, Nagoya 464-8603 (Japan)

[**] We thank Michio M. Matsushita for helpful discussions and for critical comments on this manuscript. This work was supported by a Grant-in-Aid for Scientific Research from the Ministry of Education, Culture, Sports, Science, and Technology (MEXT).

Supporting information for this article is available on the WWW under http://dx.doi.org/10.1002/anie.200900472.

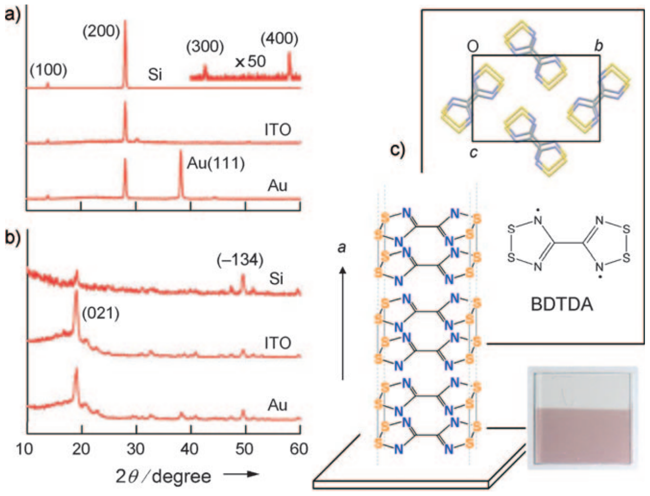

Figure 2. a) Out-of-plane and b) in-plane XRD patterns of BDTDA thin films on Si, ITO, and Au. c) Expected thin-film structure. The insets show the molecular structure of BDTDA, a photograph of a thin film on ITO, and the molecular packing of BDTDA in the *bc* plane.

oxide (ITO), and Au are shown in Figure 2a. The patterns all include periodic peaks at $2\theta = 14.0°$, $28.1°$, and so on, which correspond to an interlayer distance of 0.63 nm. This result is in agreement with the interplane distance of the *bc* plane in the bulk crystal (0.629 nm), it is thus reasonably expected that the BDTDA thin films consist of alternating π stacking perpendicular to the substrates (Figure 2c). This finding is supported by the in-plane diffractions shown in Figure 2b; these consist of several peaks that can be assigned to those from the planes of (021), (042), and so on, which are nearly perpendicular to the *bc* plane. This type of parallel molecular plane alignment has been seen in the thin films of, for instance, tetrakis(thiadiazole)porphyrazine,[17] which exhibits a layered structure that arises from electrostatic $S^{\delta+}\cdots N^{\delta-}$ contacts. However, this structure is unusual for an organic π molecule, because the perpendicular molecular plane alignment is advantageous for gaining both π-stacking stabilization and high density in the unit area of the substrates.[18] The structure of BDTDA thin films is indicative of the strong propensity of this molecule to self-assemble into the two-dimensional sheet structure in the *bc* plane, in addition to the π stacking along the *a* axis.

The ultraviolet photoelectron (UPS) and inverse photoelectron spectra (IPES) for the BDTDA thin films (10 nm) are shown in Figure S2 in the Supporting Information. The onset of the UPS spectrum occurs at around 5.37 eV, from which the threshold ionization energy I_s is determined to be (5.37 ± 0.02) eV. The threshold electron affinity A_s is determined to be (2.9 ± 0.1) eV in the solid phase from the IPES spectrum. The results of the density of state (DOS) simulations calculated for an isolated molecule and a dimer of BDTDA are also shown in Figure S2 in the Supporting Information. The experimental data are closer to the simulated DOS of the dimer rather than that of the monomer, which indicates that the electronic structure of the BDTDA thin film is also characterized by the dimerized structure.

The optical and electrical properties of the BDTDA thin films were studied. The absorption spectrum of the BDTDA thin film (100 nm) on quartz in the range 1.5–3.0 eV is shown in Figure 3a and the inset shows the data in the whole range 1.2–4.5 eV. The spectrum shows a broad band around 2.1 eV that covers the whole visible range. Molecular orbital calculations indicate that this broad band corresponds to various electronic transitions, including intramolecular, intradimer, and interdimer transitions, which are allowed in the dimeric structure of this disjoint diradical.

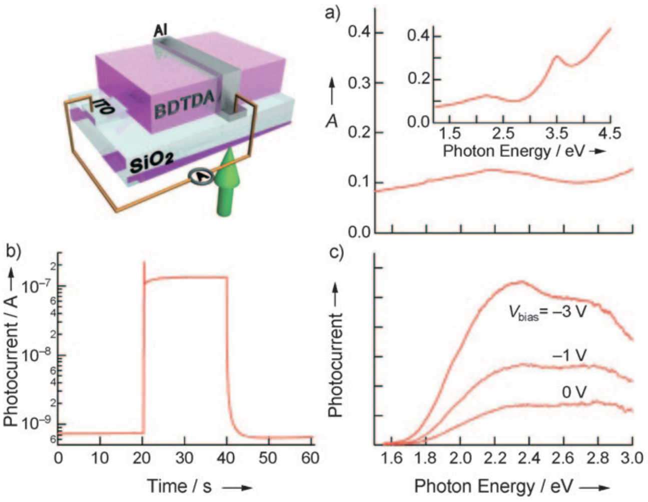

Figure 3. a) Absorption spectrum of a thin film (100 nm) of BDTDA in the range 1.5–3.0 eV. The inset shows the complete data set in the range 1.4–4.5 eV. b) On/off switching properties of the ITO/BDTDA/Al sandwich cell at a reverse bias of −3 V, exposed to a 532 nm laser under 1.59 $\mathrm{mW\,cm^{-2}}$ irradiation from the ITO side. c) The photocurrent versus the photon energy (photocurrent action spectra), taken by the ac method with $V_{bias} = -3$, -1, and 0 V.

In the dark, before irradiation, the BDTDA thin film is an insulator with a room-temperature conductivity of approximately $10^{-9}\,\mathrm{S\,cm^{-1}}$, which probably arises from the strong dimerization. To examine the photoresponse, we fabricated ITO/BDTDA/Al sandwich-type cells in which the thickness of the BDTDA layer was approximately 300 nm. The bias polarity is defined as positive when the positive bias is applied to ITO. Figure 3b shows the photocurrent induced by the illumination of a green laser (2.33 eV, 532 nm) from the ITO side with a small reverse bias voltage V_{bias} value of −3 V. The conductivity is enhanced with an on/off gain of 1.8×10^2 under an excitation light intensity of $1.59\,\mathrm{mW\,cm^{-2}}$, and the corresponding photoresponsivity is approximately $3.5\,\mathrm{mA\,W^{-1}}$. The on/off ratio increases with the light intensity and its maxima value observed in our experiments is approximately 10^3, while the photoresponsivity shows an inverse behavior and changes form 10^{-1} to $10^{-4}\,\mathrm{A\,W^{-1}}$, which is comparable to that of the most advanced organic polymer photodetectors for visible region.[19–22]

Plots of the cell photocurrent versus the photon energy (photocurrent action spectra) obtained by the ac method[23] with $V_{bias} = -3$, -1 and 0 V are shown in Figure 3c. The photocurrent is obtained across the whole range of visible light (1.8–3.0 eV), while it shows a rapid decrease below 2.2 eV. A probable explanation for this decrease is that the absorptions below 2.2 eV originate from intramolecular excitations. The wide-ranging response shown in Figure 3c is advantageous for the practical application of BDTDA to photodetectors.

It is notable that the ITO/BDTDA/Al cells produce a photocurrent even at $V_{bias} = 0$ V; this effect arises from the potential difference of the electrodes, that is, ITO (4.8 eV) and Al (4.3 eV). This photovoltaic behavior is consistent with the energy scheme based on the UPS/IPES measurements; the work functions of the two electrodes lie in the gap of the HOMO (5.37 eV) and LUMO (2.9 eV) bands of BDTDA. It is possible that the charge-separation character in the photo-excited state, that is, R^+R^-, might contribute to this photovoltaic behavior, while the mechanism of the charge separation should be studied in more detail in the future. The present results suggest possible application of the interactive radical dimers to single-component photovoltaic cells.

In summary, a disjoint diradical BDTDA forms highly oriented thin films, which are good models of interactive radical dimers; the thin films contain alternating π-stacking motifs that bridge the distance between the two electrodes. ITO/BDTDA/Al cells exhibit a photocurrent with a high on/off ratio at negative bias voltages and show photovoltaic behavior at the zero bias voltage.

Experimental Section

BDTDA was prepared as previously described.[10] The Au substrate was prepared by evaporating films (100 nm in thickness) onto glass, the Si and ITO substrates were commercially available. Before deposition, the substrates were cleaned by ultrasonic washing with acetone, 2-propanol, and chloroform. Thin films of BDTDA with thickness of 100–300 nm were prepared by vacuum vapor deposition at 190–200 °C under 4.5×10^{-4} Pa at a rate of 1–2 nm s^{-1}, using a ULVAC VPC-260FN. The film thickness was monitored during deposition by a quartz crystal microbalance located adjacent to the sample position within the bell jar. Thin-film X-ray diffraction was recorded on a Rigaku RINT2000 and SmartLab diffractometer.

The ITO/BDTDA/Al cells were fabricated by the following method: An Al electrode of 1 mm width was evaporated through a shadow mask in a vacuum with a pressure of 5×10^{-4} Pa onto BDTDA thin films deposited on an ITO electrode with a width of 2 mm. The thickness of the Al electrode was about 30 nm.

Photocurrent measurements were carried out with a 500 W halogen lamp as light source. The light, which was controlled by a shutter, was focused into a beam by a quartz lens near the output window of the Nikon G250 monochromator, in which a grating covers the 400 to 1200 nm range. The monochromated light intensity was calibrated with a Si photodiode. Two copper wires with a diameter of 100 μm were attached to the electrodes by using silver paste and then the sample was fixed into a cryostat with a pressure below 1 Pa. The transparent ITO electrode was illuminated with the monochromated light, and the photocurrent was recorded with a KEITHLEY 6487 picoammeter/voltage source. Lock-in techniques were adopted to obtain the photocurrent-action spectra. The light was chopped with a frequency of 17.0 Hz, and the signals were detected by a two phase lock-in amplifier (NF Electronic Instruments 5610B). Then photocurrent-action spectra were normalized with the photon number. Photoresponsivity (R_{res}) was calculated based on the relation $R_{res} = I_{ph}/I_{irr}\,A$, where A is the effective device area and I_{ph} and I_{irr} are the photocurrent and the incident light intensity, respectively.

Received: January 24, 2009

Keywords: organic electronics · π interactions · radicals · semiconductors · thin films

[1] S. R. Forrest, M. E. Thompson, *Chem. Rev.* **2007**, *107*, 923.

[2] H. Inokuchi, Y. Harada, Y. Maruyama, *Bull. Chem. Soc. Jpn.* **1962**, *35*, 1559.

[3] K. Awaga, T. Sugano, M. Kinoshita, *Bull. Chem. Soc. Jpn.* **1985**, *58*, 1886.

[4] X. Chi, M. E. Itkis, B. O. Patrick, T. M. Barclay, R. W. Reed, R. T. Oakley, A. W. Cordes, R. C. Haddon, *Science* **1999**, *121*, 10395.

[5] T. M. Barclay, A. W. Cordes, R. C. Haddon, M. E. Itkis, R. T. Oakley, R. W. Reed, H. Zhang, *J. Am. Chem. Soc.* **1999**, *121*, 969.

[6] T. M. Barclay, A. W. Cordes, R. H. de Laat, J. D. Goddard, R. C. Haddon, D. Y. Jeter, R. C. Mawhinney, R. T. Oakley, T. T. M. Palstra, G. W. Patenaude, R. W. Reed, N. P. C. Westwood, *J. Am. Chem. Soc.* **1997**, *119*, 2633.

[7] J. L. Brusso, K. Cvrkalj, A. A. Leitch, R. T. Oakley, R. W. Reed, C. M. Robertson, *J. Am. Chem. Soc.* **2006**, *128*, 15080.

[8] L. Beer, J. L. Brusso, A. W. Cordes, R. C. Haddon, M. E. Itkis, K. Kirschbaum, D. S. MacGregor, R. T. Oakley, A. A. Pinkerton, R. W. Reed, *J. Am. Chem. Soc.* **2002**, *124*, 9498.

[9] K. Iketaki, K. Kanai, K. Tsuboi, W. Fujita, K. Awaga, M. Knupfer, Y. Ouchi, K. Seki, *Synth. Met.* **2005**, *153*, 457.

[10] C. D. Bryan, A. W. Cordes, J. D. Goddard, R. C. Haddon, R. G. Hicks, C. D. MacKinnon, R. C. Mawhinney, R. T. Oakley, T. T. M. Palstra, A. S. Perel, *J. Am. Chem. Soc.* **1996**, *118*, 330.

[11] R. T. Oakley, *Prog. Inorg. Chem.* **1988**, *36*, 299.

[12] J. M. Rawson, A. J. Banister, I. Lavender, *Adv. Heterocycl. Chem.* **1995**, *62*, 137.

[13] J. M. Rawson, G. D. McManus, *Coord. Chem. Rev.* **1999**, *189*, 135.

[14] J. M. Rawson, F. Palacio, *Struct. Bonding (Berlin)* **2001**, *100*, 93.

[15] K. Awaga, T. Tanaka, T. Shirai, M. Fujimori, Y. Suzuki, H. Yoshikawa, W. Fujita, *Bull. Chem. Soc. Jpn.* **2006**, *79*, 25.

[16] J. M. Rawson, A. Alberola, A. Whalley, *J. Mater. Chem.* **2006**, *16*, 2560.

[17] Y. Miyoshi, M. Kubo, T. Fujinawa, Y. Suzuki, H. Yoshikawa, K. Awaga, *Angew. Chem.* **2007**, *119*, 5628; *Angew. Chem. Int. Ed.* **2007**, *46*, 5532.

[18] S. E. Fritz, S. M. Martin, C. D. Frisbie, M. D. Ward, M. F. Toney, *J. Am. Chem. Soc.* **2004**, *126*, 4084.

[19] M. C. Hamilton, S. Martin, J. Kanicki, *IEEE Trans. Electron Devices* **2004**, *51*, 877.

[20] G. A. O'Brien, A. J. Quinn, D. A. Tanner, G. Redmond, *Adv. Mater.* **2006**, *18*, 2379.

[21] Y. Xu, P. R. Berger, U. H. F. Bunz, *Appl. Phys. Lett.* **2004**, *85*, 4219.

[22] K. S. Narayan, Th. B. Singh, *Appl. Phys. Lett.* **1999**, *74*, 3456.

[23] H. Ito, Y. Niimi, A. Suzuki, K. Marumoto, S. Kuroda, *Thin Solid Films* **2008**, *516*, 2743.